Clinical Evaluation of ^{18}F-PI-2620 as a Potent PET Radiotracer Imaging Tau Protein in Alzheimer Disease and Other Neurodegenerative Diseases Compared With ^{18}F-THK-5351

Minyoung Oh, MD, PhD, Seung Jun Oh, PhD,* Sang Ju Lee, PhD,* Jungsu S. Oh, PhD,* Jee Hoon Roh, MD, PhD,† Sun Ju Chung, MD, PhD,† Jae-Hong Lee, MD, PhD,† Chong Sik Lee, MD, PhD,† and Jae Seung Kim, MD, PhD**

Purpose: PET is a useful tool for detecting the presence and extent of brain tau accumulation. However, most first-generation tau PET tracers are limited for high off-target binding and detection of tau in non-Alzheimer disease (AD). This study evaluated potential clinical applications of ^{18}F-PI-2620 as a novel PET tracer with a high binding affinity for tau deposition in AD and non-AD tauopathies.

Methods: Twenty-six participants diagnosed with either mild cognitive impairment, probable AD, frontotemporal dementia, or parkinsonism, as well as healthy controls underwent a 60- to 90-minute brain PET scan after 7 mci (259 MBq) injection of ^{18}F-PI-2620. Some participants had previous PET scans using ^{18}F-THK-5351 or ^{18}F-FP-CIT for dopamine transporter imaging.

Results: All participants showed no increase in off-target binding in basal ganglia on ^{18}F-PI-2620 PET images, as noted for first-generation tau tracers. Aβ+ mild cognitive impairment or AD patients showed diverse cortical ^{18}F-PI-2620 uptake in frontotemporoparietal cortex that correlated with Mini-Mental Status Examination ($\rho = -0.692$, $P = 0.013$). Aβ+ Parkinson disease with dementia and (Aβ unknown) primary progressive aphasia patients also showed increased ^{18}F-PI-2620 uptakes in the frontotemporoparietal cortex. Patients with parkinsonism showed increased uptakes in the pallidum compared with Aβ− healthy controls (left: 1.41 ± 0.14 vs 1.04 ± 0.13, $P = 0.014$; right: 1.18 ± 0.16 vs 0.95 ± 0.07, $P = 0.014$).

Conclusions: ^{18}F-PI-2620 PET might be a sensitive tool to detect cortical tau deposits in patients with Aβ+ AD and Aβ+ non-AD tauopathies. Furthermore, this study showed that “off-target” binding in the basal ganglia does not affect ^{18}F-PI-2620.

Key Words: tau PET, Alzheimer disease, neurodegenerative disease, off-target binding

(*Clin Nucl Med* 2020;45: 841–847)

Alzheimer disease (AD) is the most common cause of dementia, making up 60% to 80% of the cases.[1] The neuropathological hallmarks of AD are β-amyloid plaques and neurofibrillary tangles. In contrast to the early plateau of β-amyloid at the time of clinical onset and a poor correlation of β-amyloid levels with disease severity,[2] the presence and extent of neurofibrillary tangles and neuronal injury increase with disease progression.[3]

Recent developments in tau PET tracers enable in vivo imaging of pathological forms of aggregated tau in AD and non-AD tauopathies. Although several of these tracers have shown favorable pharmacokinetic profiles in vitro to tau deposits,[4] most first-generation tau PET tracers have limitations regarding high off-target binding and detection for tau in non-AD tauopathies. Next-generation tau PET tracers such as ^{18}F-PI-2620 showed improved characteristics in preclinical and in initial clinical studies.[5–7] The purpose of this study is to evaluate the potential clinical application of ^{18}F-PI-2620, a novel tau PET tracer with a high binding affinity for aggregated tau in AD and non-AD tauopathies in comparison with ^{18}F-THK-5351 PET, which is a first-generation tau PET tracer.

MATERIALS AND METHODS

Eligibility and Overall Study Design

We prospectively enrolled cognitively normal healthy controls (HCs), and patients with mild cognitive impairment (MCI), AD, frontotemporal dementia (FTD), and parkinsonism. Healthy controls were between 40 and 85 years old with no evidence of cognitive impairment by history and neuropsychological test, took a Mini-Mental Status Examination (MMSE), and scored within 1 standard deviation compared with sex, age, and education-specific norms and scored zero in clinical dementia rating (CDR). Patients with MCI met the Petersen criteria.[8] Patients with AD were older than 40 years and met the criteria for probable AD, according to the National Institute on Aging and Alzheimer's Association.[9] Diagnosis and classification of patients with FTD were defined according to the diagnostic criteria proposed by Knopman et al.[10,11] Patients with parkinsonism met each disease criteria.[12–14]

Subjects underwent amyloid PET to establish Aβ status, MRI, neuropsychological assessment including MMSE and CDR, and safety evaluation. Some of the participants had previous PET scans using ^{18}F-THK-5351.[15] ^{18}F-FP-CIT PETs were performed for all patients with parkinsonism to assess dopamine transporter (DAT) status.

All procedures performed in this study involving human participants were per the ethical standards of the institutional research committee or national research committee and with the 1964 Helsinki Declaration and its later amendments. This study was approved by the institutional review board before beginning the study. Informed consent was obtained from all participants. The clinical trial registration number is ClinicalTrials.gov Identifier: NCT03510572.

Received for publication February 27, 2020; revision accepted July 17, 2020.
From the Departments of *Nuclear Medicine, and †Neurology, Asan Medical Center, University of Ulsan College of Medicine, Seoul, South Korea.
Conflicts of interest and sources of funding: none declared.
Informed consent: written informed consent was obtained from all individual participants included in the study.
Ethics approval: all procedures performed in studies involving human participants were per the ethical standards of the institutional research committee and with the principles of the 1964 Declaration of Helsinki and its later amendments.
Authors' contributions: M.O. and J.S.K. were involved in the conception and design of the study. M.O., S.J.L., J.S.O., and S.J.O. were involved in the collection and analysis of data. J.H.R., S.J.C., J.H.L., and C.S.L. provided clinical supervision and consultation. All authors reviewed and approved the final manuscript. J.S.K. was the principal investigator.
Correspondence to: Jae Seung Kim, MD, PhD, Department of Nuclear Medicine, Asan Medical Center, University of Ulsan College of Medicine, 88, Olympic-ro 43-gil, Songpa-gu, Seoul 05505, South Korea. E-mail: jaeskim@amc.seoul.kr.

ISSN: 0363-9762/20/4511–0841
DOI: 10.1097/RLU.0000000000003261

Radiopharmaceutical Preparation of ^{18}F-PI-2620

^{18}F-PI-2620 was synthesized using a modified Trasis AllinOne automatic chemistry module according to published methods[5] with minor modifications.[16] The overall radiochemical yield was 12.1% ± 4.3% as the non–decay-corrected yield, and the total preparation time was 75 ± 5.0 minutes, including HPLC purification and formulation. The radiochemical purity and molar activity were 99.7% ± 0.6% and 46.0 ± 13.6 GBq/μmol, respectively.

PET Imaging

We acquired static brain PET scans in all participants during 60 to 90 minutes after the IV injection of 7 ± 0.7 mci (259 ± 25.9 MBq) of ^{18}F-PI-2620 for tau and 90 to 110 minutes after the IV injection of 300 ± 30 MBq of ^{18}F-florbetaben or 5 ± 0.5 mci (185 ± 18.5 MBq) of ^{18}F-flutemetamol for amyloid PET imaging using Discovery 690, 710, and 690 Elite PET/CT scanners (GE Healthcare, Boston, MA). We also acquired a static brain PET scan during 50 to 70 minutes after the IV injection of 5 ± 0.5 mci (185 ± 18.5 MBq) of ^{18}F-THK-5351 in some of the participants. Using the ordered subsets expectation maximization algorithm (iteration = 4, subset = 16), 3-dimensional (3D) PET images were reconstructed with a voxel size of 2.0 × 2.0 × 3.27 mm. We also acquired a static brain PET scan during 180 to 190 minutes after the IV injection of 185 ± 18.5 MBq of ^{18}F-FP-CIT for DAT using a Biograph truepoint 40 PET/CT scanner (Siemens USA, Washington, DC), which is reconstructed with a voxel size of 0.89 × 0.89 × 1.5 mm.

MRI Acquisition

MRI was performed with a 3.0-T system (Achieva; Philips Medical Systems, Best, the Netherlands) using an 8-channel sensitivity-encoding head coil. A high-resolution anatomical 3D volume image was obtained using a 3D gradient-echo T1-weighted sequence with the following parameters: repetition time/echo time, 9.9/4.6 milliseconds; flip angle, 8 degrees; field of view, 224 mm; matrix, 224 × 224; and slice thickness, 1 mm with no gap.

Quantitative Analysis

To measure regional uptake on ^{18}F-PI-2620 PET, we segmented 3D T1-weighted MRI scans by using the default gyral-based parcellation method of FreeSurfer (version 6.0; http://surfer.nmr.mgh.harvard.edu) using Desikan-Killiany atlas.[17] We conducted spatial coregistration of ^{18}F-PI-2620 PET onto the corresponding 3D T1-weighted MRI scans to use these volumes of interest (VOIs). Subcortical gray matter VOIs including the hippocampus, amygdala, striatum, and pallidum were also defined using the volume-based automatic FreeSurfer segmentation. The substantia nigra (SN) VOIs were defined manually on the mean image of the spatially normalized ^{18}F-PI-2620 PET images overlaid on the mean image of spatially normalized T1 MRI scans of all participants. The mean SUV ratio (SUVR) of ^{18}F-PI-2620 PET was calculated using the ^{18}F-PI-2620 uptake in these target regions over that in the inferior cerebellum (cerebellar crus b-X) as a reference region. We conducted spatial normalization of ^{18}F-PI-2620 PET (as mentioned previously, coregistered onto T1 MR first) and a FreeSurfer-based cerebellum gray matter mask to better measure the mean uptake in (pure) inferior cerebellum as a reference region. We combined these 2 masks to generate an individual-specific inferior cerebellar gray matter (CbGM) mask defined on template space. Finally, we used the morphologically eroded CbGM mask to reduce partial volume effects.

Statistical Analysis

Continuous variables were expressed as means ± standard deviations and were compared using Wilcoxon rank-sum test for changes in each group and Mann-Whitney *U* test for differences between groups. Statistical significance was defined as a 2-sided *P* value less than 0.05. Spearman correlation was performed to assess the correlation between variables. Analyses were performed using SPSS software (version 18.0; Statistical Package for the Social Science, Chicago, IL).

RESULTS

Demographics

Demographics with clinical and imaging characteristics of participants are summarized in Table 1. A total of 26 participants (mean age, 65.8 ± 7.5 years; male-to-female ratio, 16:10) included 3 HCs; 3 patients with MCI; 6 patients with probable AD including 4 with early-onset; 6 patients with FTD including 2 behavioral variant FTD (bvFTD), 3 semantic variant primary progressive aphasia (svPPA), and 1 nonfluent variant primary progressive aphasia (nfvPPA); and 8 patients with parkinsonism including 3 with corticobasal degeneration (CBD), 2 Parkinson disease with dementia (PDD), and 3 progressive supranuclear palsy (PSP). All 3 of the HCs were Aβ−, and all patients with MCI or AD (AD spectrum) were Aβ+. Among patients with FTDs, Aβ status of 1 patient with nfvPPA were unknown, and the others were Aβ−. Majority of patients with parkinsonism were Aβ− except 1 patient with PDD with Aβ+. A part of the participants had undergone ^{18}F-THK-5351 PET between 8 and 38 months before an ^{18}F-PI-2620 PET.

Visual and Quantitative Analysis of ^{18}F-PI-2620 PET

^{18}F-PI-2620 PET in AD Spectrum

Representative images of ^{18}F-PI-2620 PET are shown in Figure 1. Global SUVRs ranged from 1.01 to 1.10 in Aβ− HCs and from 0.88 to 2.64 in Aβ+ MCI and ADs (Fig. 2A). Overall, they were higher in Aβ+ groups of MCI and AD, and in one Aβ+ PDD than in Aβ− group of HC, FTD, and another parkinsonism (1.48 ± 0.49 vs 1.06 ± 0.07, $P = 0.001$). SUVRs of Braak stages I to V were numerically higher in Aβ+ MCI and ADs than in Aβ− HCs (Fig. 2B). There was a strong negative correlation between MMSE and global SUVRs in HCs and patients with MCI and AD ($\rho = -0.692$, $P = 0.013$).

As shown in Figure 1, there was no significant cortical uptake in HC on ^{18}F-PI-2620 PET, whereas mildly increased uptake in the medial temporal cortex and white matter occurred with ^{18}F-THK-5351 PET under visual inspection. In general, uptake in the medial temporal cortex were lower in ^{18}F-PI-2620 PET than ^{18}F-THK-5351 PET, regardless of the later acquisition of the former. Patients with AD spectrum showed various degrees of cortical uptakes with ^{18}F-PI-2620 PET, and it showed increased uptake not only in the cerebral cortex but also in white matter on ^{18}F-THK-5351 PET. One patient with AD showed no significant uptake in the cortex, even in the medial temporal cortex, in contrast to increased uptake in the frontotemporoparietal cortex on ^{18}F-THK-5351 PET 25 months prior.

^{18}F-PI-2620 PET in FTDs

Patients with Aβ− bvFTD or svPPA did not show a significant increase in cortical uptake with ^{18}F-PI-2620 PET, as shown in Figure 2A. One patient with bvFTD and 2 patients with svPPA had prior ^{18}F-THK-5351 PET, which showed increased uptake in the frontotemporal cortex and white matter (Fig. 3). A patient with nfvPPA showed extensive uptake in the temporal, parietal, and frontal cortex. That patient's Aβ status was unknown due to refusal to disclose the information.

TABLE 1. Demographics and Clinical and Imaging Characteristics

Group	Diagnosis/ Subject Number	Aβ (+/−)	Time From THK-5351 PET to PI-2620 PET, m	Time From FP-CIT PET to PI-2620 PET, m	Age at PI-2620 PET, y	Sex, M/F	Age at Onset, y	Education, y	Familial History	HTN	DM	Hyperlipidemia	ApoE	MMSE	CDR	CDR-SB
Normal	Normal #1	−	8		61	M		12	No	No	No	No	E3/E4	30	0	0
	Normal #2	−	9		61	F		16	No	No	No	No	E2/E3	30	0	0
	Normal #3	−			69	M		16	No	Yes	Yes	Yes		29	0	0
MCI-AD	MCI #1	+	36		82	F	78	12	No	Yes	No	Yes	E3/E4	27	0.5	2.5
	MCI #2	+	38		56	M	51	16	Yes	No	No	No	E3/E3	22	0.5	2.5
	MCI #3	+	36		69	M	63	6	Yes	Yes	No	No	E3/E4	18	0.5	4.5
	AD #1	+	25		83	F	78	6	Yes	Yes	No	No	E3/E4	20	1	5
	AD #2	+	33		71	F	64	6	Yes	Yes	No	Yes	E3/E4	20	0.5	4
	AD #3	+			71	M	63	6		No	No	No	E3/E4	23	1	7
	AD #4	+			57	M	56	6	No	No	No	No	E3/E3	18	0.5	3.5
	AD #5	+			70	M	66	16	No	No	No	No	E3/E3	10		
	AD #6	+	37		59	F	52	6	Yes	No	No	No	E3/E3	6	1	6
FTD	bvFTD #1	−			60	M	59	12	No	No	No	No	E3/E3	13	1	8
	bvFTD #2	−	26		63	F	59	12	No	Yes	No	Yes	E3/E3	7	2	11
	svPPA #1	−			57	F	54	6	Yes	Yes	No	Yes		25	0.5	
	svPPA #2	−	16		64	F	61	5	No	Yes	No	No	E3/E3	6	1	4.5
	svPPA #3	−	21		59	F	52	9	No	No	Yes	No		0	1	6
	nfvPPA #1				60	M	52	18	No	No	No	No		6	0.5	1.5
Parkinsonism	CBS/CBD #1	−		8	66	M	64	16	No	No	No	No		27		
	CBS/CBD #2	−		8	65	M	59	16	No	Yes	Yes	No	E3/E3	26	0.5	1.5
	CBS/CBD #3	−		17	65	M	56	6	No	No	No	No		26	0.5	1.5
	PDD #1	+		5	78	M	72	16	No	Yes	No	No		19	0.5	4
	PDD #2	−	14	81	73	M	60	16	No	Yes	No	No		22	0.5	3.5
	PSP #1	−		−6	59	F	56	10	No	Yes	No	No		20		
	PSP #2	−		5	63	M	58	5	No	No	Yes	No	E3/E3	29	0.5	2
	PSP #3	−		51	71	M	65	12	Yes	Yes	Yes	No		28	0	0

ApoE, apolipoprotein E; CBS, corticobasal syndrome degeneration; CBD, corticobasal degeneration; SB, sum of box; DM, diabetes mellitus; HTN, hypertension.

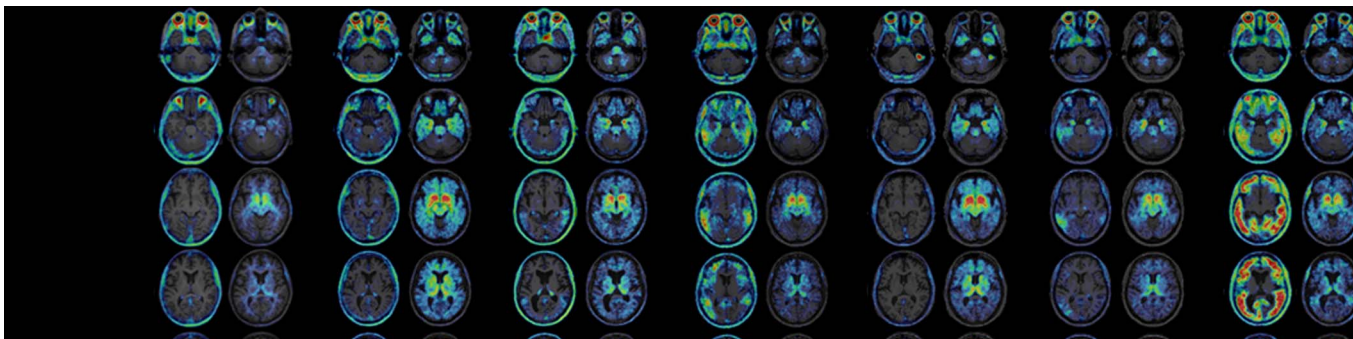

Subject No.	Normal #2 (aβ-)		MCI #1 (aβ+)		MCI #3 (aβ+)		MCI #2 (aβ+)		AD #1 (aβ+)		AD #2 (aβ+)		AD #6 (aβ+)	
Tracer	PI	THK	PI	THK	PI	THK	PI	THK	PI	THK	PI	THK	PI	THK
Age/Sex/Interval	61/F	8 m	82/F	36 m	69/M	36 m	56/M	38 m	83/F	25 m	71/F	33 m	59/F	37 m
MMSE	30	30	27	26	18	28	22	28	20	19	20	19	6	17
CDR	0	0	0.5	0.5	0.5	0.5	0.5	0.5	1	0.5	0.5	0.5	1	
CDR-SB	0	0	2.5	2	4.5	4	2.5	1.5	5	4	4	3	6	

FIGURE 1. ^{18}F-PI-2620 (PI) and ^{18}F-THK-5351 (THK) PET images of subjects with normal cognition, MCI, and AD.

^{18}F-PI-2620 PET in Parkinsonism

^{18}F-PI-2620 PET and ^{18}F-FP-CIT PET images are shown in Figure 4 in the same order of the Table 1. Uptake in the pallium for patients with parkinsonism was higher than Aβ− HCs (Fig. 2C) with statistical significance (left: 1.41 ± 0.14 vs 1.04 ± 0.13, $P = 0.014$; right: 1.39 ± 0.12 vs 0.95 ± 0.07, $P = 0.014$). It showed also higher uptakes than patients with neurodegenerative disease without parkinsonism (left: 1.41 ± 0.14 vs 1.05 ± 0.16, $P < 0.001$; right: 1.39 ± 0.12 vs 1.05 ± 0.18, $P < 0.001$). It did not correlate with disease duration ($P > 0.05$). Uptake of SN was not significantly different compared with Aβ− HCs (1.42 ± 0.20 vs 1.58 ± 0.13, $P = 0.221$ for left; 1.54 ± 0.18 vs 1.40 ± 0.20, $P = 0.307$ for right, Fig. 2D). However, it showed strong negative correlation with disease duration in patients with parkinsonism ($\rho = -0.815$, $P = 0.025$ for left; $\rho = -0.927$, $P = 0.003$ for right).

One of the patients with CBD showed asymmetric uptakes in the pallidum and SN. It showed an asymmetrical decrease of striatal DAT binding on ^{18}F-FP-CIT PET, which corresponds with the right side–dominant parkinsonism of the patient.

Off-Target Binding of ^{18}F-PI-2620 PET

There was no significant increase in uptake in the basal ganglia on ^{18}F-PI-2620 PET, as seen with ^{18}F-THK-5351 PET (Fig. 1). Uptakes in choroid plexus, cerebral venous sinus, scalp, extraocular, and temporalis muscles were observed occasionally. Increased uptake in the retina was observed in all cases. Uptake on meningioma was observed on both ^{18}F-PI-2620 PET and ^{18}F-THK-5351 PET in 1 patient with AD in the right tentorium cerebelli.

Some of the participants showed increased uptake in the anterior lobe of the cerebellum regardless of their clinical diagnosis, as shown in Figure 2E. Uptake for SN was variable among participants (Fig. 2D).

DISCUSSION

This study provides preliminary results of ^{18}F-PI-2620 PET for imaging tau protein depositions in AD and other neurodegenerative diseases. The study showed various degrees of cortical uptake expected in Braak staging in the AD spectrum and also showed increased cortical uptake in Aβ+ PDD and Aβ unknown nfvPPA with advanced AD-like pattern. No significant uptake was observed in patients with Aβ− bvFTD and Aβ− svPPA, which showed characteristic increased uptake in the frontotemporal cortex on the earlier ^{18}F-THK-5351 PET. In patients with parkinsonism, the uptake in the pallium increased slightly, and the uptake in SN gradually decreased with longer disease duration. We also demonstrated that no off-target binding is observed in the basal ganglia, which indicates monoamine oxidase-B (MAO-B) by direct comparison with ^{18}F-THK-5351 PET, a first-generation tau tracer.[18]

In this study, most patients with Aβ+ MCI or AD showed higher cortical uptakes compared with Aβ− HCs on ^{18}F-PI-2620 PET and reached up to 3.0 in terms of global and regional SUVR. The study showed gradually increasing degrees of cortical uptake as cognitive impairment worsens after a known distribution of tau deposition according to Braak histopathological staging, and it showed strong negative correlation with MMSE scores.[19] Although direct comparison is complicated due to interindividual variance and difference of PET acquisition, reconstruction, and quantification, it seems that high contrast images in AD compared with HCs are similar to AV-1451 and other second-generation tau PET tracers.[20–22]

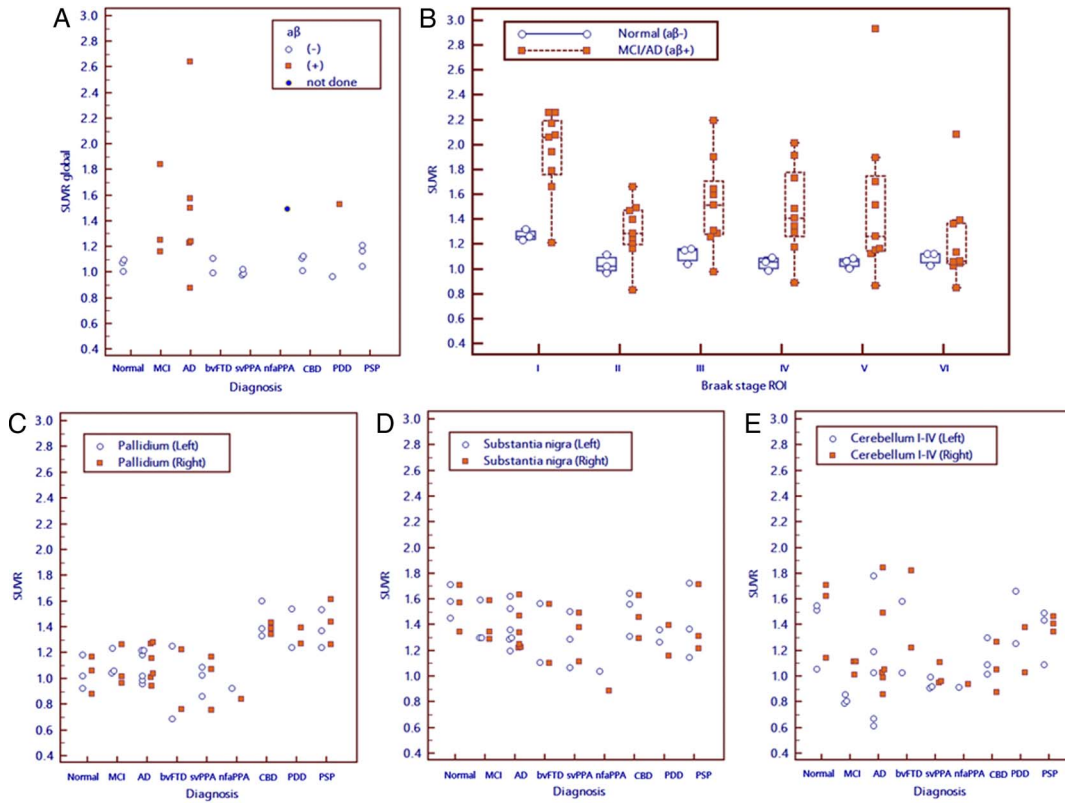

FIGURE 2. **A**, Global ^{18}F-PI-2620 SUVRs of all participants according to Aβ status. **B**, SUVRs of Braak stages I to VI in AD spectrum. SUVRs of the pallium (**C**), substantia nigra (**D**), and cerebellum I to IV (**E**) of all participants.

One patient with AD, however, showed no significant uptake in the cerebral cortex in ^{18}F-PI-2620 PET, including medial temporal cortex nevertheless of Aβ+, and increased uptake in the overall cortex in ^{18}F-THK-5351 PET scan done 25 months ago. Furthermore, this patient showed predominant atrophy in the bilateral temporal cortex, including the hippocampus, on MRI. Her MMSE score was 20 at the time of ^{18}F-PI-2620 PET. Botha et al[23] showed medial temporal and posterior cingulate hypometabolism regardless of Aβ status in patients with tau-negative amnestic dementia, whereas lateral parietal and inferior temporal hypometabolism is predominant in typical AD on FDG PET. Autopsies of these patients revealed hippocampal sclerosis.

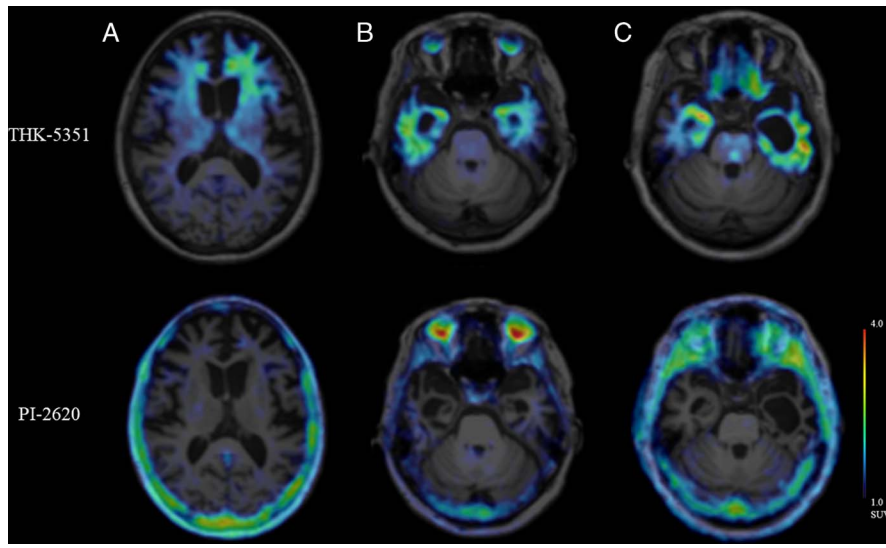

FIGURE 3. ^{18}F-THK-5351 (upper row) and ^{18}F-PI-2620 PET images of patients with Aβ– bvFTD #2 (**A**) and Aβ– svPPA #2 and #3 (**B** and **C**).

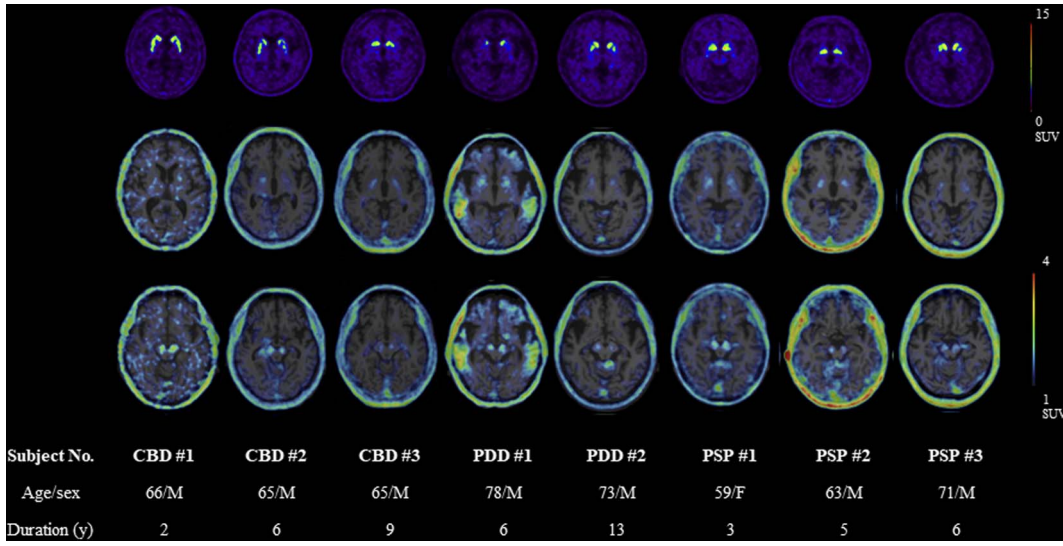

FIGURE 4. ^{18}F-FP-CIT PET (upper row) and ^{18}F-PI-2620 PET (middle and lower rows) images of patients with CBD #1 to #3, PDD #1 and #2, and PSP #1 to #3.

Tau PET imaging for parkinsonism has been a challenge. First, straight or twisted ribbon tau filaments are more common in patients with parkinsonism compared with predominant paired helical filaments of tau in AD mainly targeted in currently available tau PET tracers.[24] Second, off-target binding of ^{18}F-THK-5351 and ^{18}F-AV-1451 is a hurdle in identifying tau in the basal ganglia, which is known as a tau-rich area in patients with parkinsonism. In this study, we showed increased uptake in the pallidum in patients with CBD, PDD, and PSP. In a patient with CBD who showed asymmetric striatal ^{18}F-FP-CIT binding, uptake in the pallidum on ^{18}F-PI-2620 PET was asymmetric and reflected asymmetric patterns of symptoms that are specific for CBD. This case shows the potential of ^{18}F-PI-2620 PET for non-AD tau imaging, although we did not confirm this by pathology. As reported recently, for non-AD tauopathies, it may be advantageous to use dynamic scanning from 0 to 60 minutes postinjection.[25]

Tau protein deposits in SN of the midbrain are frequently found in patients with parkinsonism, including PSP.[26] However, almost all first-generation tau PET tracers showed increased uptake to melanin-containing cells found in SN.[27] Therefore, it is recommended that PET tracers targeting such diseases avoid binding to melanin-containing cells, but this is not achievable with current technology. In patients with parkinsonism, in this study, we showed a duration-dependent decreased uptake in SN (Fig. 4). An explanation for this finding is cell death caused by tau deposition-induced disease progression, but studies with large sample size and autopsy follow-up are needed for more assurance.

In terms of off-target binding, ^{18}F-PI-2620 PET showed no significant uptake increase in the basal ganglia in contrast to ^{18}F-THK-5351 PET. According to recent reports about the cross-interaction between the first- and second-generation tau PET tracers and MAO-B, ^{18}F-PI-2620 PET is one of the tau PET tracers that had the lowest values for binding to MAO-B,[28] which is partly explained by its low molar volume, which does not favor interaction with the binding site on the MAO-B. This study also showed no significant uptake of ^{18}F-PI-2620 in the cortex and white matter observed on ^{18}F-THK-5351 PET and other studies with the first-generation of tau PET tracers.[15,29] Although FTDs represents a heterogeneous clinical, genetic, and pathological entity, the majority of Aβ− svPPA is likely to be TDP43 proteinopathy.[30] Despite that, it is still controversial whether ^{18}F-THK-5351 uptake reflects neuroinflammation identified by MAO-B or another kind of unrevealed nonspecific binding; negative uptake in this category gives better specificity for tau in ^{18}F-PI-2620 PET.

^{18}F-PI-2620 PET, however, showed variable degrees of nonspecific binding in the choroid plexus, cerebral venous sinus, facial and extraocular muscles, scalp, and retina as seen in other tau PET tracers.[31–33] Incidental uptake in meningioma was also observed in ^{18}F-PI-2620 PET and ^{18}F-THK-5351 PET in a patient with AD. It was reported that meningioma could show increased uptake of first-generation tau PET tracers.[34] The mechanism of uptake is not clear, but it is not known to accumulate tau protein.

We choose eroded inferior CbGM as a reference for quantification because it provides small individual differences among participants in this study. The use of the whole CbGM can be complicated as a reference region for ^{18}F-PI-2620 PET caused by variable uptake in the anterior cerebellum (vermis) in the participants, regardless of disease type. Although it was not observed on the ^{18}F-THK-5351 PET scans of our participants (Fig. 1), it seems to be found in second-generation tau PET tracers, including ^{18}F-MK-6240 and ^{18}F-RO-948.[35,36] Further study is needed to evaluate the etiology of the uptake in the anterior cerebellum in second-generation tau PET tracers. There is also a chance that the binding of the anterior cerebellum is specific for tau in patients with PSP.[26,37] Furthermore, the study showed nonspecific and variable binding in the cerebral venous sinus that can interfere with uptakes in the cerebellar cortex in the anterior lobe and even in the superior part of the posterior lobe.

One of the limitations of this study is the small sample size, but this initial clinical evaluation provides insight into the performance of ^{18}F-PI-2620 as a tau PET tracer in variable neurodegenerative disease. Second, time intervals between ^{18}F-PI-2620 PET and ^{18}F-THK-5351 PET are long and difficult for direct comparison. However, all ^{18}F-THK-5351 PET scans were acquired before ^{18}F-PI-2620, and time interval is relatively constant in patients with MCI and AD. In addition, it provides enough evidence to prove no off-target binding in the basal ganglia, which represents nonspecificity for tau in ^{18}F-THK-5351 PET. Another limitation of this study is the lack of reliable clinical measurements, including PSP scores in patients with parkinsonism. Instead, we collected disease duration as an indirect measure of disease severity, and all patients with parkinsonism

demonstrated variable degrees of DAT loss on ^{18}F-FP-CIT PET, which can provide objective evidence of degenerative parkinsonism.[38,39]

CONCLUSIONS

^{18}F-PI-2620 PET might be a sensitive tool to detect tau deposits in patients with Aβ+ AD and Aβ+ non-AD tauopathies. Furthermore, this study showed that "off-target" binding in the basal ganglia does not affect ^{18}F-PI-2620. Further studies with larger sample sizes are needed to evaluate further ^{18}F-PI-2620 binding in Aβ-tauopathy.

ACKNOWLEDGMENTS

This research was supported by Life Molecular Imaging GmbH (formerly Piramal Imaging GmbH, Berlin, Germany) and a grant of the Korea Health Technology R&D Project through the Korea Health Industry Development Institute (KHIDI), funded by the Ministry of Health & Welfare, Republic of Korea (grant number: HI14C2768 and HI18C2383).

REFERENCES

1. Alzheimer's Association. 2018 Alzheimer's disease facts and figures. *Alzheimers Dement*. 2018;14:367–429.
2. Giannakopoulos P, Herrmann F, Bussière T, et al. Tangle and neuron numbers, but not amyloid load, predict cognitive status in Alzheimer's disease. *Neurology*. 2003;60:1495–1500.
3. Gómez-Isla T, Hollister R, West H, et al. Neuronal loss correlates with but exceeds neurofibrillary tangles in Alzheimer's disease. *Ann Neurol*. 1997; 41:17–24.
4. Brosch JR, Farlow MR, Risacher SL, et al. Tau imaging in Alzheimer's disease diagnosis and clinical trials. *Neurotherapeutics*. 2017;14:62–68.
5. Kroth H, Oden F, Molette J, et al. Discovery and preclinical characterization of [(^{18})F]PI-2620, a next-generation tau PET tracer for the assessment of tau pathology in Alzheimer's disease and other tauopathies. *Eur J Nucl Med Mol Imaging*. 2019;46:2178–2189.
6. Mueller A, Bullich S, Barret O, et al. Tau PET imaging with (^{18})F-PI-2620 in patients with Alzheimer's disease and healthy controls: a first-in-human study. *J Nucl Med*. 2020;61:911–919.
7. Bullich S, Barret O, Constantinescu C, et al. Evaluation of dosimetry, quantitative methods and test-retest variability of (18)F-PI-2620 PET for the assessment of tau deposits in the human brain. *J Nucl Med*. 2020;61:920–927.
8. Petersen RC, Smith GE, Waring SC, et al. Aging, memory, and mild cognitive impairment. *Int Psychogeriatr*. 1997;9(Suppl 1):65–69.
9. McKhann GM, Knopman DS, Chertkow H, et al. The diagnosis of dementia due to Alzheimer's disease: recommendations from the National Institute on Aging-Alzheimer's Association workgroups on diagnostic guidelines for Alzheimer's disease. *Alzheimers Dement*. 2011;7:263–269.
10. Rascovsky K, Hodges JR, Knopman D, et al. Sensitivity of revised diagnostic criteria for the behavioural variant of frontotemporal dementia. *Brain*. 2011;134:2456–2477.
11. Gorno-Tempini ML, Hillis AE, Weintraub S, et al. Classification of primary progressive aphasia and its variants. *Neurology*. 2011;76:1006–1014.
12. Armstrong MJ, Litvan I, Lang AE, et al. Criteria for the diagnosis of corticobasal degeneration. *Neurology*. 2013;80:496–503.
13. Litvan I, Agid Y, Calne D, et al. Clinical research criteria for the diagnosis of progressive supranuclear palsy (Steele-Richardson-Olszewski syndrome): report of the NINDS-SPSP international workshop. *Neurology*. 1996;47:1–9.
14. McKeith IG, Boeve BF, Dickson DW, et al. Diagnosis and management of dementia with Lewy bodies: fourth consensus report of the DLB consortium. *Neurology*. 2017;89:88–100.
15. Son HJ, Oh JS, Roh JH, et al. Differences in gray and white matter 18 F-THK5351 uptake between behavioral-variant frontotemporal dementia and other dementias. *Eur J Nucl Med Mol Imaging*. 2019;46:357–366.
16. Lee SJ, Hyun JS, Oh SJ, et al. Development of a new precursor-minimizing base control method and its application for the automated synthesis and SPE purification of [^{18}F] fluoromisonidazole ([^{18}F] FMISO). *J Label Compd Radiopharm*. 2013;56:731–735.
17. Fischl B, Salat DH, Busa E, et al. Whole brain segmentation: automated labeling of neuroanatomical structures in the human brain. *Neuron*. 2002;33: 341–355.
18. Ng KP, Pascoal TA, Mathotaarachchi S, et al. Monoamine oxidase B inhibitor, selegiline, reduces (18)F-THK5351 uptake in the human brain. *Alzheimers Res Ther*. 2017;9:25.
19. Braak H, Braak E. Staging of Alzheimer's disease-related neurofibrillary changes. *Neurobiol Aging*. 1995;16:271–278; discussion 278–284.
20. Schwarz AJ, Yu P, Miller BB, et al. Regional profiles of the candidate tau PET ligand ^{18}F-AV-1451 recapitulate key features of Braak histopathological stages. *Brain*. 2016;139:1539–1550.
21. Maass A, Landau S, Baker SL, et al. Comparison of multiple tau-PET measures as biomarkers in aging and Alzheimer's disease. *Neuroimage*. 2017; 157:448–463.
22. Lois C, Gonzalez I, Johnson KA, et al. PET imaging of tau protein targets: a methodology perspective. *Brain Imaging Behav*. 2019;13:333–344.
23. Botha H, Mantyh WG, Murray ME, et al. FDG-PET in tau-negative amnestic dementia resembles that of autopsy-proven hippocampal sclerosis. *Brain*. 2018;141:1201–1217.
24. Whitwell JL. Tau imaging in parkinsonism: what have we learned so far? *Mov Disord Clin Pract*. 2018;5:118–130.
25. Brendel M, Barthel H, Van Eimeren T, et al. ^{18}F-PI2620 tau-PET in progressive supranuclear palsy: a multi-center evaluation. *Alzheimers Dement*. 2019;15:P128–P129.
26. Williams DR, Holton JL, Strand C, et al. Pathological tau burden and distribution distinguishes progressive supranuclear palsy-parkinsonism from Richardson's syndrome. *Brain*. 2007;130:1566–1576.
27. Marquie M, Normandin MD, Vanderburg CR, et al. Validating novel tau positron emission tomography tracer [F-18]-AV-1451 (T807) on postmortem brain tissue. *Ann Neurol*. 2015;78:787–800.
28. Murugan NA, Chiotis K, Rodriguez-Vieitez E, et al. Cross-interaction of tau PET tracers with monoamine oxidase B: evidence from in silico modelling and in vivo imaging. *Eur J Nucl Med Mol Imaging*. 2019;46:1369–1382.
29. Josephs KA, Martin PR, Botha H, et al. [(18) F]AV-1451 tau-PET and primary progressive aphasia. *Ann Neurol*. 2018;83:599–611.
30. Seelaar H, Rohrer JD, Pijnenburg YA, et al. Clinical, genetic and pathological heterogeneity of frontotemporal dementia: a review. *J Neurol Neurosurg Psychiatry*. 2011;82:476–486.
31. Tago T, Toyohara J, Harada R, et al. Characterization of the binding of tau imaging ligands to melanin-containing cells: putative off-target-binding site. *Ann Nucl Med*. 2019;33:375–382.
32. Ikonomovic MD, Abrahamson EE, Price JC, et al. [F-18]AV-1451 positron emission tomography retention in choroid plexus: more than "off-target" binding. *Ann Neurol*. 2016;80:307–308.
33. Lemoine L, Leuzy A, Chiotis K, et al. Tau positron emission tomography imaging in tauopathies: the added hurdle of off-target binding. *Alzheimers Dement (Amst)*. 2018;10:232–236.
34. Bruinsma TJ, Johnson DR, Fang P, et al. Uptake of AV-1451 in meningiomas. *Ann Nucl Med*. 2017;31:736–743.
35. ALZFORUM. Move over, flortaucipir? New tau tracers tested in people. Available at: https://www.alzforum.org/news/research-news/move-over-flortaucipir-new-tau-tracers-tested-people#enlarge. Accessed October 24, 2019.
36. Wong DF, Comley RA, Kuwabara H, et al. Characterization of 3 novel tau radiopharmaceuticals, (11)C-RO-963, (11)C-RO-643, and (18)F-RO-948, in healthy controls and in Alzheimer subjects. *J Nucl Med*. 2018;59: 1869–1876.
37. Piao YS, Hayashi S, Wakabayashi K, et al. Cerebellar cortical tau pathology in progressive supranuclear palsy and corticobasal degeneration. *Acta Neuropathol*. 2002;103:469–474.
38. Oh M, Kim JS, Kim JY, et al. Subregional patterns of preferential striatal dopamine transporter loss differ in Parkinson disease, progressive supranuclear palsy, and multiple-system atrophy. *J Nucl Med*. 2012;53:399–406.
39. Han S, Oh M, Oh JS, et al. Subregional pattern of striatal dopamine transporter loss on ^{18}F FP-CIT positron emission tomography in patients with pure akinesia with gait freezing. *JAMA Neurol*. 2016;73:1477–1484.